



Atomic layer deposition of multicomponent amorphous oxide semiconductors with sequential dosing of metal precursors

Jong Beom Ko ^a, Sang-Hee Ko Park ^{b,*}

^a Department of Materials Science and Engineering, Hanbat National University, Daejeon, 34158, Republic of Korea

^b Department of Materials Science and Engineering, Korea Advanced Institute of Science and Technology, 291 Daehak-ro, Yuseong-gu, Daejeon 34141, Republic of Korea

ARTICLE INFO

Keywords:

Amorphous oxide semiconductor
Atomic layer deposition
Multicomponent
Thin-film transistors

ABSTRACT

Atomic layer deposition (ALD) is a suitable method for depositing amorphous oxide semiconductors (AOSs) because it has the potential for achieving high performance in complex structures owing to its excellent step coverage and atomic-scale controllability. Multicomponent AOSs are typically deposited using the ALD with a super-cycle method. In this study, multicomponent AOSs, i.e., IZO, ITO, and ITZO, were deposited using ALD by employing a sequential dosing of metal precursors. Their compositions were adjusted by varying the dose time of the indium precursor. Subsequently, we applied the IZO, ITO, and ITZO films in thin-film transistors (TFTs), which demonstrated normal transfer characteristics. The TFT containing ITZO with 73.9 at% indium exhibited a turn-on voltage of -1.01 V, subthreshold swing of 0.09 V/dec, and field-effect mobility of 35.9 $\text{cm}^2/(\text{V s})$.

1. Introduction

Amorphous oxide semiconductors (AOSs) are considered promising candidates for advanced display driver devices owing to several benefits, including high mobility and uniformity over large areas [1]. A mixture of two or more cations with different atomic sizes and ionic charges is required to create an amorphous phase in oxide semiconductors [2]. Multicomponent AOS films are typically deposited using sputtering. However, it is difficult to apply these films to three-dimensional (3D) structures such as vertical channels [3]. In contrast, atomic layer deposition (ALD) is a superior method for depositing thin films with excellent uniformity and step coverage. This allows for precise thickness control and yields high-quality films through self-limiting surface growth [4]. Consequently, ALD has attracted significant attention for AOS deposition in thin-film transistors (TFTs). Multicomponent AOSs are typically deposited using a super-cycle approach, which involves the deposition of different mono-oxide layers. The film composition can be adjusted by modifying the number of unit cycles for each component. However, this approach leads to form polycrystalline mono-oxide layers owing to a heterogeneous distribution of the depth profile [5].

In this study, we deposited various types of indium (In)-based multicomponent AOSs, i.e., IZO, ITO, and ITZO, by sequentially dosing metal precursors to form a monolayer of multicomponent layers. The composition is affected by the steric hindrance of precursors; therefore,

the sequence of precursor exposure must be carefully considered. To facilitate the deposition of multicomponent AOSs, we started the dosing from a precursor with a large ligand size followed by precursors with smaller ligand sizes, thereby ensuring that unoccupied sites [6]. Furthermore, the composition of the AOS was modulated by varying the dose time of the In precursors. The electrical characteristics of the TFTs were evaluated.

2. Experiment section

The multicomponent AOS was deposited using plasma-enhanced ALD (PEALD) at 250 °C. $\text{Et}_2\text{InN}(\text{SiMe}_3)_2$, Et_3Sn , and Et_2Zn were used as the In, Sn, and Zn precursors, respectively. The reactive gas (O_2) was utilized with a plasma power of 100 W. The PEALD sequence is shown in Fig. 1. In the deposition of AOSs, the dose times for the Zn and Sn precursors were fixed at 0.2 and 0.5 s, respectively, and the In precursor was injected under two different conditions (0.5 and 1.0 s) to modify the composition. X-ray photoelectron spectroscopy (XPS) and X-ray diffraction (XRD) were used for composition analysis and microstructure characterization, respectively. The PEALD-processed AOS films were incorporated into the active layer of TFTs with a bottom-gate bottom-contact structure, and their electrical properties were investigated. In TFT fabrication, ITO served as the gate and source/drain electrode, Al_2O_3 formed a 170 nm gate insulator (GI) via thermal-ALD at 150 °C.

* Corresponding author.

E-mail address: shkp@kaist.ac.kr (S.-H.K. Park).

<https://doi.org/10.1016/j.matlet.2024.136297>

Received 18 October 2023; Received in revised form 8 March 2024; Accepted 11 March 2024

Available online 12 March 2024

0167-577X/© 2024 Elsevier B.V. All rights reserved.

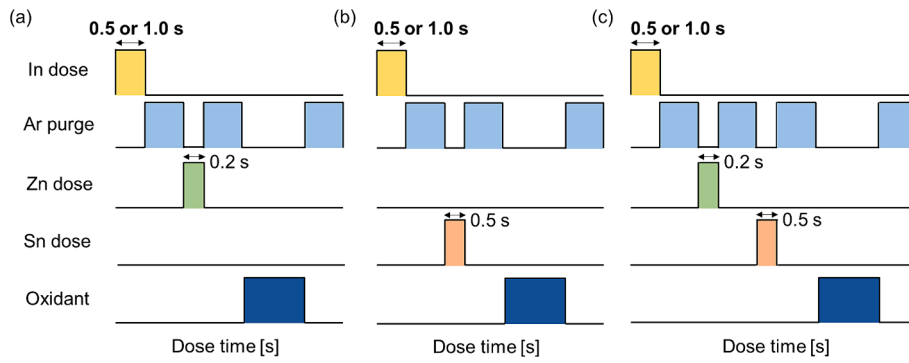


Fig. 1. Schemes of ALD sequences for the deposition of (a) IZO, (b) ITO, and (c) ITZO films.

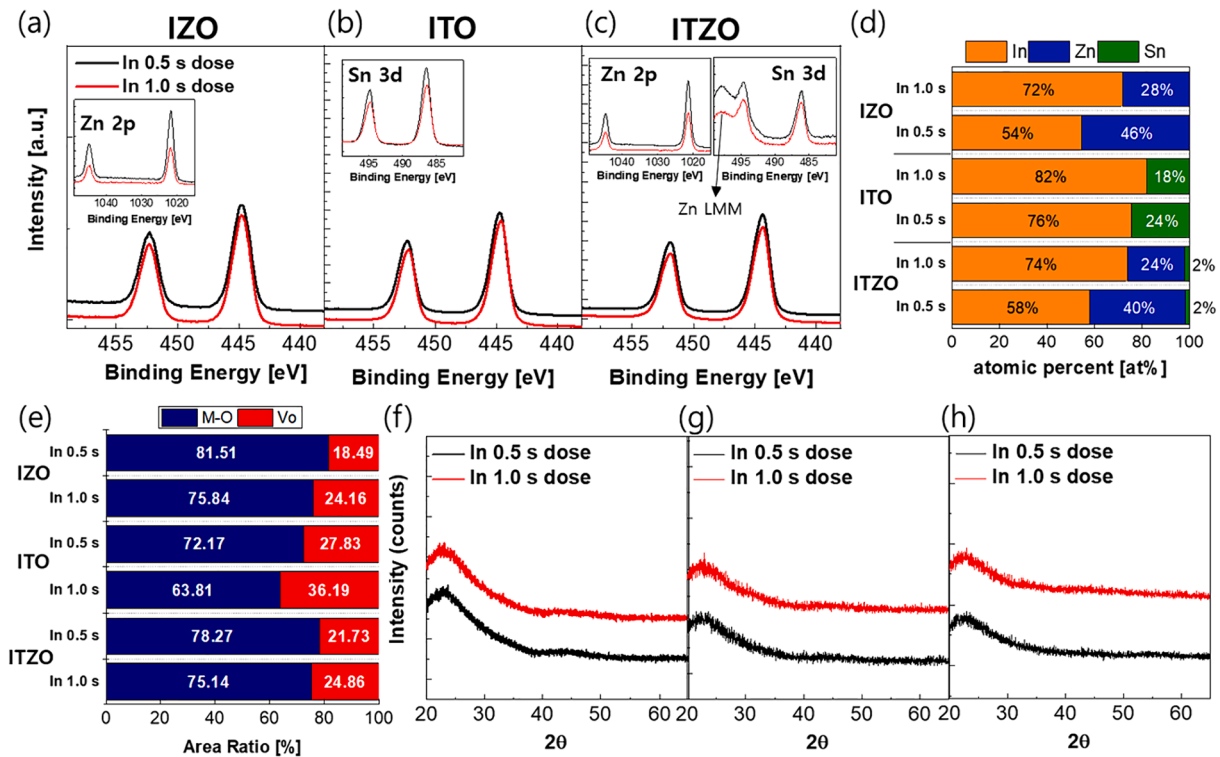


Fig. 2. XPS spectra for In 3d peaks of PEALD-processed (a) IZO, (b) ITO, and (c) ITZO (inset: Zn and Sn peaks), and (d) extracted atomic percentage of PEALD-processed AOSs. (e) Peak area ratio between M–O and Vo in O1s peaks. XRD patterns of (f) IZO, (g) ITO, and (h) ITZO.

10 nm thick of IZO, ITO, and ITZO were deposited as the active using PEALD. The TFTs were annealed in an O₂ environment at 350 °C to rectify defects. For the devices with ITO active layer, an additional plasma treatment was conducted using N₂O at 130 W for 30 s to adjust the carrier density. To ensure passivation, a 100 nm thick layer of SiO₂ was deposited using PECVD at 300 °C. Finally, the devices underwent thermal annealing in vacuum at 300 °C to cure remaining defects.

3. Results and discussion

Fig. 2 (a), (b) and (c) shows the In 3d peaks identified in the XPS spectra of the AOS films deposited using PEALD. The XPS results clearly indicate the presence of In in the AOS thin films. It should be noted that the IZO and ITO films exhibit distinct peaks corresponding to Zn and Sn, respectively. In addition, the ITZO film exhibits Zn and Sn peaks, as shown in the inset of Fig. 2. The composition is obtained from the area of the metal peaks and summarized in Fig. 2 (d). The In content in the AOS increases with the dose time of the In precursor. This shows that the

composition can be modified by controlling the precursor dose times. It should be noted that the Sn content in ITZO is lower than that in ITO, even with the same dose times of In and Sn precursors. It can be inferred that an additional dose of the Zn precursor reduces the number of unoccupied sites, which could have been filled by the Sn precursor, thereby reducing the Sn content in the ITZO film.

The phases of the PEALD-processed AOSs are investigated using XRD. As shown in Fig. 2 (f), (g) and (h), all the AOS films display a broad pattern without any sharp peaks, indicating that the films maintain an amorphous phase even with a large amount of In. In the super-cycle method, it is challenging to increase the content of a single element owing to thick host oxide layers that impede vertical intermixing [5]. Therefore, the deposition of AOS films with the sequential dosing of metal precursors provides the advantage of achieving a high atomic ratio of a single element in the AOS films while maintaining the amorphous phase.

The PEALD-processed AOSs are employed as the active layers in the TFTs, and their transfer characteristics are evaluated at a drain voltage

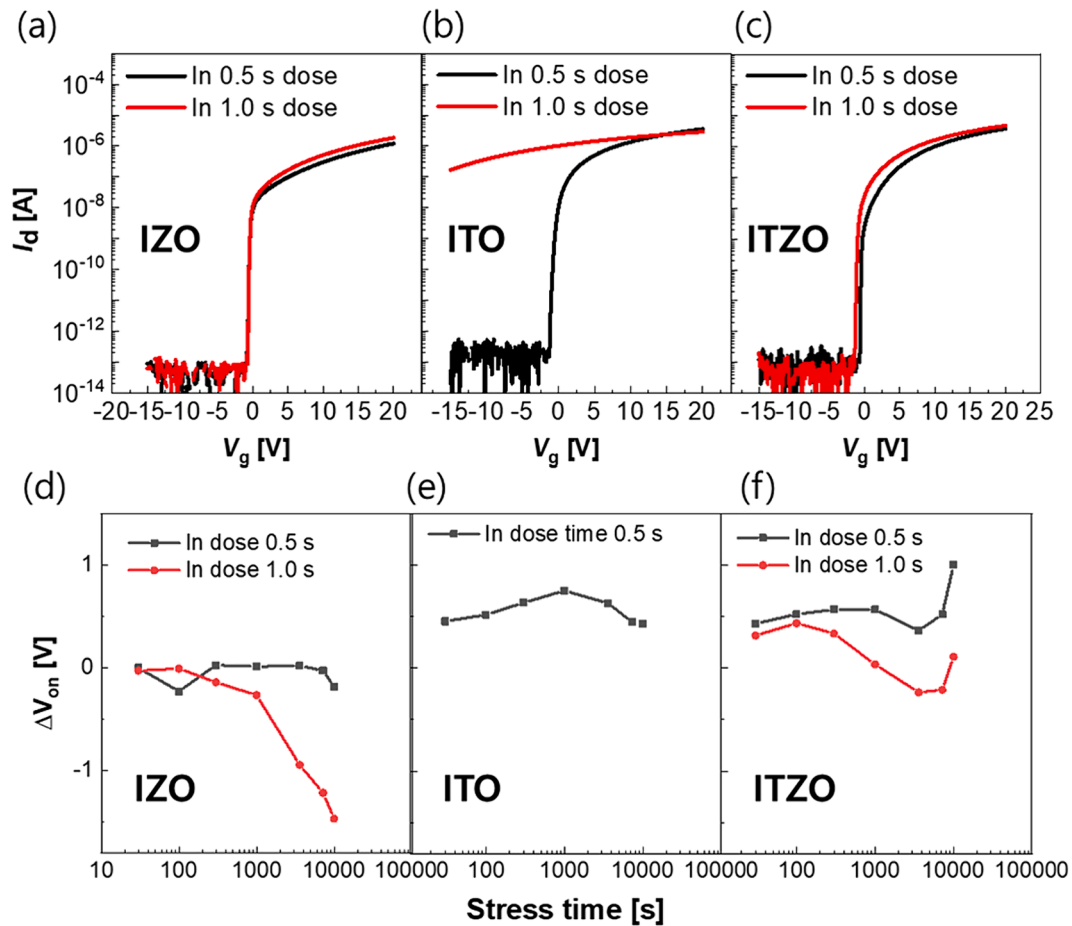


Fig. 3. Transfer curves of TFTs with PEALD-processed (a) IZO, (b) ITO, and (c) ITZO. ΔV_{on} under PBTS for the TFTs with (d) IZO, (e) ITO, and (f) ITZO.

Table 1
Electrical Parameters of TFTs with PEALD-processed AOSs.

Materials	In dose time [s]	V_{on} [V]	Mobility [cm^2/Vs]	S.S [V/dec.]
IZO	0.5	-0.56 ± 0.03	13.0 ± 1.8	0.07 ± 0.01
	1.0	-0.60 ± 0.12	22.6 ± 0.9	0.09 ± 0.01
ITO	0.5	-1.00 ± 0.13	27.3 ± 4.6	0.16 ± 0.05
	1.0	N/A	N/A	N/A
ITZO	0.5	-0.54 ± 0.16	33.7 ± 2.0	0.09 ± 0.01
	1.0	-1.01 ± 0.26	35.9 ± 1.5	0.09 ± 0.01

of 0.1 V. The width and length of the devices are 40 and 20 μm , respectively. As depicted in Fig. 3 (a), (b) and (c), the TFTs exhibit typical transfer curves; the electrical parameters are summarized in Table 1. As the In dose time increases, the field-effect mobility increases and the turn-on voltage (V_{on}) exhibits a negative shift. It is widely acknowledged that In plays a significant role in AOSs by influencing the current path and carrier generation by augmenting V_o as shown in Fig. 2 (e) [7]. The TFT with the ITO active exhibits conductor-like behavior as the In content increases, because, ITO is a well-known conducting oxide containing a substantial number of intrinsic carriers. Furthermore, the TFT with ITZO exhibits notable improvements in mobility even though its In content is similar to that of the TFT with IZO. Prior research has indicated that relatively heavy metal cations, particularly Sn, deepen the conduction band minimum, leading to increased conduction band dispersion, effective carrier doping, and reduced effective mass [4]. Consequently, the addition of even a small amount of Sn to the AOS results in a significant improvement in the mobility.

The stability under positive bias temperature stress (PBTS) is

investigated with a stress gate voltage of 20 V at 60 $^{\circ}\text{C}$ for 10,000 s. The ΔV_{on} under PBTS for each device is depicted in Fig. 3 (d), (e) and (f). All devices exhibit abnormal behavior during PBTS. In this study, the devices exhibit a negative shift at certain stress times. Previous studies have shown that H diffuses into AOSs in the form of H^+ under PBTS, causing a negative shift in V_{on} by generating excess carriers when a H-rich GI is used [8]. Thermal-ALD-processed Al_2O_3 , which is used as the GI in this study, contains a high concentration of H because H_2O is used as a reactant [9]. Consequently, the devices exhibit abnormal behaviors during PBTS. When investigating ΔV_{on} to compare defect states, the ΔV_{on} either becomes more positive or less negatively shifted as the In content decreases. Instability under PBTS is generally attributed to electron-trapping sites closely associated with oxygen interstitial (Oi) in AOSs [9]. The weak bonding between In and O induce the generation of oxygen deficiencies. Thus, as the In content increases, there is a compensating effect on Oi, leading to a decrease in ΔV_{on} in the positive direction [7].

4. Conclusions

Various multicomponent AOS films were deposited using PEALD with the sequential dosing of metal precursors. PEALD-processed IZO, ITO, and ITZO distinctly exhibited multiple compositions with an amorphous phase, even with a high In content. The compositions of the AOS films were adjusted by varying the In precursor dose time. PEALD-processed AOSs were employed as the active layers in TFTs, which exhibited reasonable transfer characteristics. In particular, TFTs with PEALD-processed ITZO containing 73.9 at% In exhibited a field-effect mobility of $35.9 \text{ cm}^2/(\text{Vs})$. Further optimization of the fabrication

process, such as the deposition conditions for GIs and device structure, is necessary to ensure the performance of the devices and examine their characteristics. Nevertheless, there is potential for application in 3D structured electronic devices with a wide range of compositions.

CRedit authorship contribution statement

Jong Beom Ko: Conceptualization, Data curation, Formal analysis, Investigation, Visualization, Writing – original draft. **Sang-Hee Ko Park:** Funding acquisition, Writing – review & editing.

Declaration of competing interest

The authors declare that they have no known competing financial interests or personal relationships that could have appeared to influence the work reported in this paper.

Data availability

Data will be made available on request.

Acknowledgements

This work was supported by the Technology Innovation Program Development Program (1415185633, Development of high reliability light emitting fiber based woven wearable display) funded By the Ministry of Trade, Industry & Energy (MOTIE, Korea)

References

- [1] J.S. Park, W.J. Maeng, H.S. Kim, J.S. Park, Review of recent developments in amorphous oxide semiconductor thin-film transistor devices, *Thin Solid Films* 520 (2012) 1679–1693, <https://doi.org/10.1016/j.tsf.2011.07.018>.
- [2] T. Kamiya, H. Hosono, Material characteristics and applications of transparent amorphous oxide semiconductors, *NPG Asia Mater.* 2 (2010) 15–22, <https://doi.org/10.1038/asiamat.2010.5>.
- [3] D.H. Kim, K.H. Lee, S.H. Lee, J. Kim, J. Yang, J. Kim, S.I. Cho, K.H. Ji, C.S. Hwang, S. H.K. Park, Trench-structured high-current-driving aluminum-doped indium–tin–zinc oxide semiconductor thin-film transistor, *IEEE Electron. Dev. Lett.* 43 (2022) 1677–1680, <https://doi.org/10.1109/LED.2022.3201072>.
- [4] J.Z. Sheng, J.H. Lee, W.H. Choi, T. Hong, M. Kim, J.S. Park, Review article: atomic layer deposition for oxide semiconductor thin film transistors: advances in research and development, *J. Vac. Sci. Technol. A* 36 (2018), <https://doi.org/10.1116/1.5047237>.
- [5] M. Coll, M. Napari, Atomic layer deposition of functional multicomponent oxides, *APL Mater.* 7 (2019), <https://doi.org/10.1063/1.5113656>.
- [6] C.T. Nguyen, B. Gu, T. Cheon, J. Park, M.R. Khan, S.H. Kim, B. Shong, H.B.R. Lee, Atomic layer modulation of multicomponent thin films through combination of experimental and theoretical approaches, *Chem. Mater.* 33 (2021) 4435–4444, <https://doi.org/10.1021/acs.chemmater.1c00508>.
- [7] J. Sheng, T. Hong, H.M. Lee, K. Kim, M. Sasase, J. Kim, H. Hosono, J.S. Park, Amorphous IGZO TFT with high mobility of similar to 70 cm²/(Vs) via vertical dimension control using PEALD, *ACS Appl. Mater. Interfaces* 11 (2019) 40300–40309, <https://doi.org/10.1021/acsami.9b14310>.
- [8] S.I. Cho, J.B. Ko, S.H. Lee, J. Kim, S.H.K. Park, Remarkably stable high mobility self-aligned oxide TFT by investigating the effect of oxygen plasma time during PEALD of SiO₂ gate insulator, *J. Alloys Compd.* 893 (2022), <https://doi.org/10.1016/j.jallcom.2021.162308>.
- [9] J.B. Ko, S.I. Cho, S.H.K. Park, Engineering a subnanometer Interface tailoring layer for precise hydrogen incorporation and defect passivation for high-end oxide thin-film transistors, *ACS Appl. Mater. Interfaces* 15 (2023) 47799–47809, <https://doi.org/10.1021/acsami.3c10185>.